Astron. Astrophys. 309, 633–647 (1996)

ASTRONOMY AND ASTROPHYSICS

Discovery of solid formaldehyde toward the protostar GL 2136: observations and laboratory simulation*

W.A. Schutte[1], P. A. Gerakines[1,2], T.R. Geballe[3], E.F. van Dishoeck[1], and J.M. Greenberg[1]

[1] Leiden Observatory, P.O. Box 9513, 2300 RA Leiden, The Netherlands
[2] Department of Physics, Rensselaer Polytechnic Institute, Troy, NY 12180-3590, USA
[3] Joint Astronomy Centre, 660 N. A'ohoku Pl., Hilo, HI 96720, USA

Received 6 July 1995 / Accepted 13 October 1995

Abstract. A search for the ν_5 band of solid formaldehyde toward the protostellar source GL 2136 has resulted in the detection of absorption features near 3.47 and 3.54 μm. A good match of the 3.47 μm feature exists with solid H_2CO features in laboratory analogs of interstellar ice condensates. The abundance of H_2CO and the composition of the ice in which it is found are constrained by the precise wavelength of the 3.47 μm absorption, the profile of the 3.54 μm absorption feature, and the previously observed 9.75 (CH_3OH), 6.0, and 6.8 μm features. From comparison with laboratory spectra, we conclude that the H_2CO and CH_3OH are intimately mixed and that both contribute to the 3.54 μm absorption, while the profiles of the 6.0 and 6.8 μm bands indicate a contribution of the solid H_2CO ν_2 and ν_3 features at 5.8 and 6.7 μm. We estimate that the abundance of H_2CO is ~ 7 % of that of H_2O seen along the same line of sight, but that only a small fraction of the H_2O is intimately mixed with the H_2CO. There appear to be at least two types of ice mantles present along the line of sight, one consisting of almost pure H_2O (type I ice) and the other rich in, if not dominated by H_2CO and CH_3OH (type II ice). The possible origin of solid H_2CO and the implication of our results for the physical and chemical conditions in the cloud are discussed

Key words: ISM: clouds – ISM: dust, extinction – ISM: molecules – stars: individual: GL 2136 – methods: laboratory – infrared: ISM: lines and bands

1. Introduction

One of the most salient aspects of dense cloud chemistry is the accretion and subsequent processing of molecules on interstellar grains. Inside clouds the time scale for a molecule to collide with a grain is of the order of 10^5 years at typical densities of $n_H = 10^4$ cm^{-3} (e.g., Schutte & Greenberg 1991; Schutte 1996). With grain temperatures of $\sim$ 10 K (Greenberg 1971; Mathis et al. 1983), all molecules and atoms more massive than He will stick to the grain at nearly 100 % efficiency (e.g., Tielens & Allamandola 1987a). Thus, grains collect an icy mantle consisting of a mixture of species. Upon accretion, the molecules can be modified by reactions with atoms and light radicals such as H, O, C, N and their partially hydrogenated counterparts, which are able to diffuse over the grain surface (Tielens & Hagen 1982; Hasegawa et al. 1992, Hasegawa & Herbst 1993a). Furthermore, the ices may be photochemically modified, leading to the production of more complex and/or unstable species (Greenberg 1973; Greenberg 1979; d'Hendecourt et al. 1986; Allamandola et al. 1988; Grim et al. 1989; Shalabiea & Greenberg 1994).

In view of the short accretion timescales, mantle desorption mechanisms must exist for maintaining the observed gaseous material inside dense clouds, for example heating by cosmic rays or explosive release of stored chemical energy (Greenberg 1976; Greenberg 1979; Léger et al. 1985; d'Hendecourt et al. 1982; Schutte & Greenberg 1991). Thus, processes taking place on the grains will influence the cloud chemistry in its entirety. The chemical conditions in dense clouds can therefore only be understood if solid and gas phase processes are considered as parts of a complete chemical system synthesized by the interaction through accretion and desorption. The H_2CO molecule is a particularly sensitive tracer of this interaction, since, while abundantly observed in the gas phase, it is believed to be primarily formed on grains (Federman & Allen 1991; Shalabiea & Greenberg 1994).

In the special case that a young stellar object is present inside the dense cloud molecules can be returned to the gas phase also by thermal evaporation or shock processes due to the interaction of the stellar outflow and the dense core. Gas–phase reactions will subsequently modify the chemical composition through ion–molecule or neutral–neutral reactions. Therefore, the molecular composition of the grain mantles and the gas reflect the evolutionary state of the young stellar object (Blake

Send offprint requests to: W.A. SCHUTTE

* Based on observations collected by the United Kingdom Infrared Telescope at Mauna Kea, Hawaii, and by the New Technology Telescope at the European Southern Observatory, La Silla, Chile

et al. 1987; Charnley et al. 1992; Caselli et al. 1993; Helmich et al. 1994).

The composition of ice mantles in interstellar clouds can be studied by observing the infrared absorption features of obscured sources, which can be either embedded young stellar objects or background field stars. Interpretation of these features is achieved through comparison with laboratory simulations in which interstellar ice analogs are prepared through slow deposition of gases on a cold ($\sim$ 10 K) substrate, and monitored in situ by infrared spectroscopy. In this way a considerable number of species have been identified in the icy mantles, i.e., H_2O, CO, CH_3OH, H_2, OCS and possibly CO_2 and CH_4 (e.g.; reviews by Whittet 1993; van Dishoeck et al. 1993; Schmitt 1994; Schutte 1996).

Theoretical models predict that formaldehyde (H_2CO) is an important constituent of the icy mantles, due to the grain surface hydrogenation of the abundant gas constituent CO (Tielens & Hagen 1982; Hasegawa et al. 1992; Hasegawa & Herbst 1993) Furthermore, solid formaldehyde can be produced by ultraviolet photolysis of H_2O– and CO– containing ice mantles (Zhao 1990, Shalabiea & Greenberg 1994). Indirect evidence for the presence of formaldehyde in the ice mantles can be derived from observations of gas in the Orion compact ridge and hot core. In these warm regions, associated with massive star formation, the mantles evaporate. The observed high abundances of H_2CO and its reaction product $HCOOCH_3$ can only be explained in terms of injection from the grain mantles (Blake et al. 1987; Charnley et al. 1992). Additionally, the very high deuterium fractionation of the formaldehyde strongly suggests that the initial formation of this molecule took place on the grain mantles (Turner 1990). More generally, models of purely gas phase chemical processes fall short in reproducing the observed quantity of gaseous formaldehyde in translucent and dense clouds. It was therefore proposed that formaldehyde production on grains in combination with "non–thermal" desorption events accounts for the bulk of H_2CO also in general molecular clouds (Greenberg 1979; Federman & Allen 1991; Shalabiea & Greenberg 1994).

Solid H_2CO has a number of infrared absorption features. Fig. 1 shows the spectrum of pure H_2CO ice at 10 K. The positions and vibrational modes (from Pugh & Rao 1976) of the most intense features are indicated. For a full listing of the positions and band strengths of solid H_2CO we refer to Schutte et al. (1993). The ν_2 and ν_3 vibrational modes give strong features at 5.80 and 6.69 μm, respectively, in a region accessible only to space or airborne observations, leaving just the weaker bands at 3.47 and 3.54 μm, due to the ν_5 and ν_1 modes, respectively, to ground–based observation. However, attempts to observe these features toward the embedded massive protostars W33 A, NGC7538 IRS9 and W3 IRS5 failed (Grim et al. 1991; Allamandola et al. 1992). Although a feature at 3.54 μm was observed toward the first two of these objects, there was no sign of a band near 3.47 μm, thus excluding an assignment to H_2CO. Instead the 3.54 μm feature was assigned to the ν_3 mode of solid methanol (CH_3OH).

The 5 to 8 μm region, encompassing the strongest of the formaldehyde bands, was observed at very low resolution by the Kuiper Airborne Observatory (KAO; Tielens & Allamandola 1987b; Tielens 1989). This region is generally dominated by broad absorption features at 6.0 μm and 6.8 μm. The former is ascribed to solid H_2O (e.g., Tielens & Allamandola 1987b), while the latter feature has not yet been satisfactorily identified (cf; overviews by Whittet 1993; Schutte 1996). Comparing the 6.0 and 6.8 μm features of the embedded sources W33A and NGC7538 IRS9 with those of GL 2136, it is found that both GL 2136 features are somewhat broadened and redshifted. It was shown that this difference could be caused by the presence of the formaldehyde bands near 5.8 and 6.7 μm (Schutte 1988), indicating that substantial amounts of solid H_2CO may be present toward this source. However, the low resolution of the airborne observations precluded a secure identification.

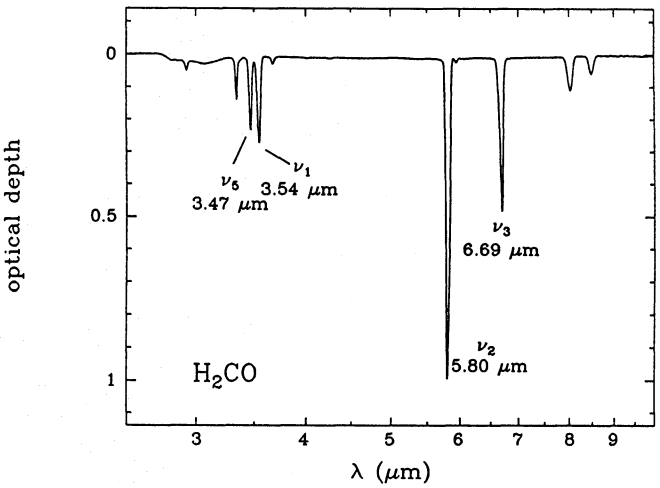

Fig. 1. Infrared spectrum of solid H_2CO deposited on a 10 K substrate

This paper reports the results of a search for the ν_5 and ν_1 absorption features of solid H_2CO near 3.47 and 3.54 μm toward GL 2136 with the United Kingdom Infrared Telescope (UKIRT) at Mauna Kea, Hawaii, and the New Technology Telescope (NTT) of the European Southern Observatory at La Silla, Chile. The UKIRT spectrum shows two absorption features centered near 3.47 and 3.54 μm. Although the noise level as well as telluric methane structure is much larger in the NTT spectrum, these observations are also consistent with the presence of these bands.

The 3.47 μm band is observed for the first time. Based on comparison with spectra of astrophysical ice analogs, we propose an identification of this feature with solid formaldehyde. The 3.54 μm band was observed previously toward other embedded sources and has been identified as the ν_3 feature of solid methanol (CH_3OH; Grim et al. 1991; Allamandola et al. 1992). The ν_1 H_2CO mode would also contribute to this feature in GL 2136.

The paper is laid out as follows. In Sect. 2 we describe the observational techniques and present the obtained spectroscopic data. Sect. 3 presents the identification of the GL 2136 3.47 μm absorption with solid H_2CO by comparing this band and the 3.54 μm feature to spectra of laboratory ices containing H_2CO and CH_3OH. In Sect. 4 we summarize the spectroscopic data ob-

Table 1. Summary of observations of GL 2136

Telescope	Range μm	Date	t_{int} s
UKIRT	3.38–3.58	1993 March 7	128
UKIRT	3.57–3.77	1993 March	14360
NTT	3.40–3.68	1994 March	28240

tained for a number of formaldehyde– and methanol–containing laboratory ice samples prepared for comparison with these features. A basic interpretation of the spectroscopic results in terms of the physical–chemical properties of the ices is given. Sect. 5 explores the composition of the interstellar H_2CO–containing ice by studying the requirements for matching the observations. Sect. 6 discusses the origins of solid H_2CO in dense clouds, and the implications of our results for the ambient chemical conditions. Our conclusions are summarized in section 7.

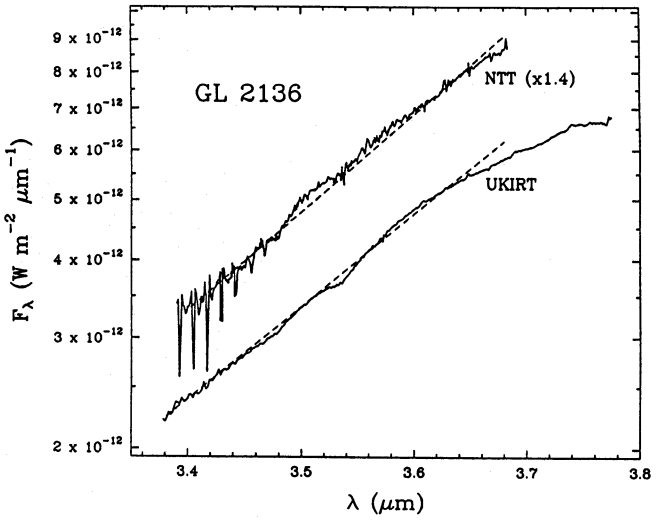

Fig. 2. High resolution spectroscopy ($\lambda/\Delta\lambda \approx 1200$) of GL 2136 obtained by UKIRT and the NTT. For clarity, fluxes have been multiplied by 1.4 for the NTT data. The baselines applied to obtain optical depth plots (Fig. 3) are given by dashed lines

2. Observations

Parameters for the various observing runs are given in Table 1. Spectroscopy between 3.38 and 3.77 μm was obtained with the United Kingdom Infrared Telescope (UKIRT) on Mauna Kea, using CGS4, a cryostat containing a grating spectrometer and a 58x62 pixel SBRC array. The plate scale was 1.54"/pixel and the width entrance slit to the spectrometer corresponded to 1.54". A 300 lines/mm grating was used in first order, producing a resolving power ($\lambda/\Delta\lambda$) of approximately 1100 in the above wavelength range. The observations were made in the chop/nod mode, with the chopper throw equivalent to 10 rows of the array. Wavelength calibration was achieved using an argon lamp in second order; the accuracy of the wavelength scale is better than 0.001 μm.

Additional 3.40 – 3.68 μm spectroscopy was obtained with the New Technology Telescope (NTT) at the European Southern Observatory using IRSPEC, a cryogenically cooled grating spectrometer equipped with a 58 x 62 pixel SBRC InSb array. Grating 1 having 300 lines mm^{-1} in first order was used, providing a spectroscopic resolving power of $\lambda/\Delta\lambda$ = 1600. Sky subtraction was readily obtained with the 2 dimensional detector array which allows simultaneous measurement of the object and nearby sky. Nodding over a distance of 60" in declination was performed every minute, producing sky observations on opposite sides of the object. Wavelength calibration was achieved with a neon lamp at an accuracy better than 0.001 μm.

Both the UKIRT and NTT data were flux calibrated and corrected for telluric absorption by ratioing with the standard star BS 6378 (spectral type A2 V). The resulting spectrum was flux–calibrated using L=2.31 for this star (Glass 1974) and a spectral shape of a 9000 K black body. In the UKIRT data, a small mismatch in air–mass between object and standard was corrected by a small continuum subtraction and scale–up of the standard star spectrum. For the NTT data, the difference in airmass between object and standard was small and correcting for this difference (for example, by using a second standard star at different air mass; Schutte et al. 1991) did not improve the results beyond the simple ratioing of the object with standard measurements, due to the relatively great amount of the telluric absorption at the telescope site.

Fig. 2 shows the UKIRT and NTT spectra of GL 2136. The two spectra are generally consistent, apart from a set of narrow absorptions in the 3.4 – 3.5 μm region in the NTT spectrum, which are due to incomplete cancellation of telluric CH_4 lines. The spectra are characterized by a steep red slope, caused by the strong 3 μm feature of H_2O ice and its associated long wavelength shoulder and the emission spectrum of the source (Willner et al. 1982). Two relatively weak, narrow, features appear to be superimposed on the slope. To highlight these features, we subtracted a straight line in the $\log(F_\lambda)$–λ plane which was fitted through the regions 3.38 – 3.43 μm and 3.62 – 3.64 μm. It should be emphasized that this procedure does not in any way represent a "true" continuum subtraction, as residual structure associated with the red shoulder will still be present, and should only be regarded as a cosmetic operation which enables a clearer view of the weaker features. It is important to note that any baseline definition should be performed in the $\log(F_\lambda)$–λ plane rather than in the F_λ–λ plane, since the latter procedure introduces spurious structure in the resulting optical depth plots, since straight lines in the F_λ–λ plane may be strongly curved in the $\log(F_\lambda)$–λ plane.

The resulting "optical depth" plots give a more clear view of the two narrow features (Fig. 3). Also shown are the spectra after smoothing to a resolution of 0.008 μm. Only the smoothed version of the NTT results is displayed because of the high noise level of the original data. To obtain the intrinsic wavelength, the spectra were corrected for a small Doppler shift by adding 2 x 10^{-4} μm to the original wavelength scale. This shift was obtained from the Local Standard of Rest velocity of the gas

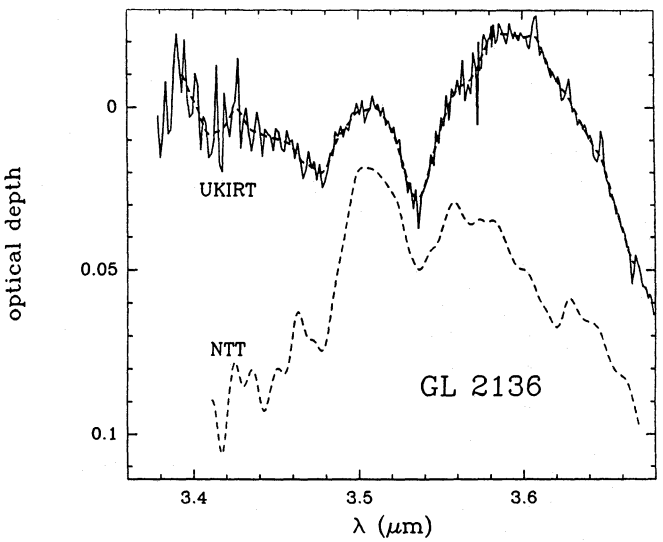

Fig. 3. "Optical depth" plots obtained from the UKIRT and NTT spectroscopy (Fig. 2) by subtracting a straight baseline. Besides the unsmoothed spectrum (resolution 0.003 μm; solid line), the spectra after smoothing to 0.008 μm resolution are also shown (dashed lines). Because of its high noise level, only the smoothed version is shown of the NTT spectrum. For clarity, the NTT spectrum has been shifted downward by 0.06 units. The displayed spectra have been corrected for the Doppler shift by adding 2 x 10^{-4} μm to the original wavelength scale (see text)

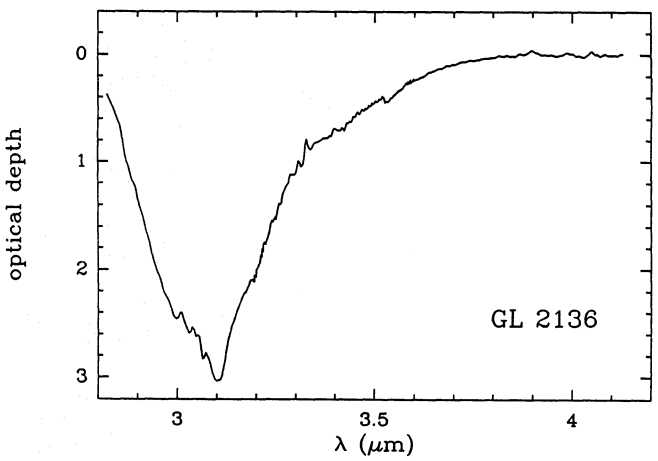

Fig. 4. Optical depth plot of the 3 μm solid water feature toward GL 2136. This plot was obtained from the original flux data by subtracting a third order polynomial fit of the continuum (see text)

associated with GL 2136 of 27 km s^{-1} which corresponds to a heliocentric velocity of 12 km s^{-1}, and the velocity component due to the earth orbital motion of -28 km s^{-1} at the time of the UKIRT and NTT observations. The UKIRT spectrum shows two narrow features at 3.4743 $\pm$ 0.002 μm and 3.5358 $\pm$ 0.0015 μm (Henceforth the "3.47" and "3.54" μm bands). Similar structure appears to be present in the NTT spectra. Despite the longer integration time, the NTT data are of considerably less quality than the UKIRT data. This is due to the less favorable site, i.e., lower altitude, which results in a higher sky background and larger telluric absorption features. This is most evident in the region of telluric methane below 3.46 μm. The detection of the 3.47 μm band in the NTT spectrum by itself would hardly be significant, in view of apparent spurious structure of almost similar intensity near, for example, 3.62 μm. However, considered in combination with the UKIRT data, the NTT provides some confirmation of the existence of this band. Because of its superior quality, we will base our analysis of the ice features toward GL 2136 exclusively on the UKIRT spectrum.

To complement the new data, Fig. 4 displays earlier lower resolution data from 2.8 to 4.2 μm μm encompassing the 3 μm feature of solid H_2O. Segments of the 3-4 micron low resolution spectrum of GL 2136 were obtained at UKIRT on UT 1983 July 25 (3.18 – 3.53 μm), 26 (2.83 – 3.23 μm), and 28 (3.53 – 4.18 μm) at UKIRT, utilizing CGS2, a seven-channel cold grating spectrometer, operating at a resolving power of ~400. The aperture diameter was 5" and a 30 arcsecond east-west chop and nod were employed. The spectral segments each were sampled every 1/2 resolution element. The integration time per point was 40 seconds for the shortest wavelength segment and 20 seconds for the other two. Wavelength calibration was achieved using an argon arc lamp observed in second order. Correction for telluric features was obtained by ratioing the GL2136 spectra by spectra of BS6638, BS6658, and BS6698, stars of spectral types G and K. The spectra of these stars may contain weak molecular absorption lines in the 3-4um region; therefore, the existence of weak and narrow spectral structures in the reduced spectrum of GL2136 should be regarded with caution. The three spectral segments were scaled slightly in flux density over their common spectral intervals and then adjoined to produce the final spectrum. The optical depth plot of the water feature in Fig. 4 was obtained by subtracting a third order polynomial representation of the continuum from the original data. The polynomial was fitted through the spectral regions 2.2 – 2.7 μm and 3.8 – 4.2 μm. The shorter wavelength continuum region was adapted from Willner et al. (1982), after normalizing our data set to that of Willner et al. using the region of overlap between 3.8 – 4.2 μm. Alternatively a black–body fit through the continuum regions was attempted which however resulted in a relatively poor match. Indeed the continuum flux resulting from a superposition of emission from grains at various temperatures along the line of sight convolved with the wavelength dependent grain emission efficiency is not expected to necessarily resemble black body emission, justifying the more general polynomial fitting procedure.

3. Solid formaldehyde toward GL 2136

The 3.54 μm band has been previously observed toward other protostellar objects and has been identified with solid methanol (Grim et al. 1991; Allamandola et al. 1992). The presence of this feature is no surprise, since solid methanol has previously been detected toward GL 2136 by its ν_8 feature at 9.75 μm (Skinner et al. 1992). The 3.47 μm band, on the other hand, has not yet been seen toward other obscured sources. While very broad absorption structure (FWHM $\approx$ 0.15 μm) associated with the

red shoulder of the interstellar water ice band is generally found in this spectral region (e.g., Allamandola et al. 1992 made a tentative assignment of this structure to interstellar diamonds), it must be emphasized that the new 3.47 μm band, having FWHM ≤ 0.03 μm, is clearly distinct from this broad structure, and, up to this time, has only been observed toward GL 2136.

In an initial assessment, the detection of the 3.47 μm feature toward GL 2136 seems consistent with the presence of solid H_2CO indicated by the KAO 5 – 8 μm spectrum (Schutte 1988; see below). In this interpretation, the new feature should be assigned to the H_2CO ν_5 band. For a 10 K deposit of pure formaldehyde ice this feature peaks at 3.467 μm (e.g, Schutte et al. 1993), well shortward of the observed 3.47 μm feature. However, laboratory spectroscopy of formaldehyde in various ice matrices has shown that the position of the ν_5 feature varies considerably, from 3.448 μm in a CO_2 matrix to 3.494 μm when diluted in CO ice (van der Zwet et al. 1985). The ν_1 mode falls consistently ~ 0.076 μm longward of the ν_5 band. Thus, if the observed 3.474 μm feature is caused by formaldehyde ice, the ν_1 band is expected to fall at ~ 3.550 μm. Its width and intensity should be comparable to that of the ν_5 band (van der Zwet et al. 1985). It therefore appears likely that this second H_2CO feature is blended with the solid methanol 3.54 μm feature, preventing a clear detection.

To test whether the 3.47 μm feature could be caused by solid formaldehyde, we prepared a number of astrophysical ice analogs in the laboratory, searching for a good match of the GL 2136 data. A full report of our experimental results is presented in section 4. Here we restrict ourselves to those results that specifically support the identification of solid H_2CO. The possible range of ice conditions that can be used in our search of parameter space is constrained by earlier observations of the infrared bands of various ice components toward GL 2136. The deduced column densities and average composition of the ice along the line of sight are listed in table 2. Furthermore, the shape and position of the absorption features give important information on the physical and chemical conditions of the ices. Fits to the solid CO band show that all CO toward GL 2136 is embedded in polar ice, presumably H_2O (Tielens et al. 1991). Fits to the 9.75 μm methanol band show that the methanol ice is mixed with at most ~ 1.5 times as much H_2O, far less than the ratio of the column densities (Skinner et al. 1992; Table 2). It thus appears that CH_3OH and the bulk of the H_2O ice reside in separate phases of the icy mantles.

To make a useful comparison with GL 2136, a reasonable temperature average must be taken over the spectra of the interstellar ice analogs. The H_2O band toward GL 2136 falls at 3.103 μm (Fig. 4), indicating relatively high ice temperatures (Smith et al. 1989; Hagen et al. 1981). Its position and shape is similar to the water band of the BN object. The latter feature was reproduced by a superposition of the feature of H_2O ice at different temperatures, at a ratio of 23 K:77 K:150 K = 3.1:1.2:1.0 (Smith et al. 1989). The GL 2136 feature is positioned slightly longward of the BN band, i.e., 3.103 μm vs. 3.095 μm, indicating that the average temperature of the ice along the line of sight is some 20 – 30 K warmer than toward BN (Hagen et al. 1981). The absence of solids dominated by apolar species also indicates $T_{dust} \gtrsim 30$ K along most of the line of sight (Sandford et al. 1988). Unless diluted in an overabundance of refractory water ice, i.e., H_2O:$H_2CO \gtrsim 10$:1, formaldehyde ice evaporates above ~ 115 K (Schutte et al. 1993). Therefore the bulk of the ices toward GL2136 that could contain H_2CO should have temperatures in the range 40 – 110 K, with an average perhaps near 70 K. For this reason, we used in all cases a temperature average of the laboratory spectra at a ratio of 50K:70K:100K = 2:4:1 for comparison with GL 2136.

Table 2. Summary of ice components observed toward GL 2136

Species	Feature μm	Column Density cm^{-2}	Abundance	Ref
H_2O	3.1	5.0(18)[a]	100	1
CO	4.68	1.8(17)[b]	3.6	2
CH_3OH	3.54	[2.0 ± 0.5](17)	4.0±1.0	1
	9.7	[3.9 ± 1.5](17)		3
H_2CO	3.47	[3.1 ± 1.3](17)	6.2±2.7	1
	5.8/6.7		9.6±2	1
CO_2	15.2	$\leq$ 5.0(16)[c]	≤ 1	4
XCN	4.62	$\leq$ 2.7(16)[d]	≤ 0.5	5

[a]Using A = 2.1 x 10^{-16} cm, for water ice at 70 K (Gerakines et al. 1995). [b]Using A = 1.0 x 10^{-17} cm, for CO embedded in water ice at 70 K (Gerakines et al. 1995). [c]Using A = 1.1 x 10^{-17} cm (Gerakines et al. 1995). [d]Using A = 7.0 x 10^{-17} cm (Grim et al. 1989). References: 1. This paper 2. Tielens et al. 1991; 3. Skinner et al. 1992; 4. Whittet & Walker 1991; 5. Geballe 1986.

Fig. 5 shows the best laboratory fit, corresponding to the ice mixture H_2O:CH_3OH:H_2CO = 3.7:2.0:3.1 (Henceforth "the standard mixture"). The composition of this sample is consistent with the abundance ratio of $[CH_3OH]/[H_2O] \gtrsim 0.6$ for the methanol–containing ices as deduced from the 9.75 μm feature (Skinner et al. 1992). It can be seen that the standard mixture provides good fits to both the 3.47 and 3.54 μm features. Moreover, it shows two relatively shallow features at 3.377 and 3.408 μm. Although the short wavelength end of the spectrum suffers from interference of telluric methane, still some corresponding structure seems distinguishable in the GL 2136 spectrum. As will be discussed in Sect. 4, the appearance of these features is a general property of ice mixtures of CH_3OH and H_2O. For comparison, Fig. 5 also shows the spectrum of the mixture H_2O:CH_3OH = 3.7:2.0. Comparing the laboratory spectra, it can be seen that the presence of the ν_1 formaldehyde mode underlying the ν_3 methanol band introduces a shallow red shoulder on the 3.54 μm feature. Although this seems to somewhat decrease the quality of the fit to the GL 2136 band, the presence of very broad underlying structure associated with the red shouder of the solid water 3 μm band may account for this apparent discrepancy. This is illustrated by Fig. 6 which shows the residual obtained by subtracting the spectrum of the standard mixture from GL 2136. The residual should represent the underlying broad structure associated with the red shoulder. For

comparison, the spectrum of the embedded protostellar object W3 IRS5 is also shown (from Allamandola et al. 1992). This spectrum was obtained from the original data of Allamandola et al. (1992) after the same baseline subtraction procedure was applied as for GL 2136 (Sect. 2). W3 IRS5 shows no sign of the 3.54 and 3.47 μm absorption features, so that any structure in its spectrum should originate from the broad shoulder absorption. It can be seen that similar structures are present in the GL 2136 residual and the W3 IRS5 spectrum; i.e., a steep downward slope longwards of 3.56 μm, and a broad absorption structure centered at $\sim$ 3.48 μm. These structures can be considered part of the red shoulder absorption, after its appearance has been modified by the baseline subtraction procedure; i.e., no absorption features other than the well–known shoulder need to be invoked to account for the W3 IRS5 spectrum and the GL 2136 residual in Fig. 6. Thus we conclude that, within the limits set by the underlying structure of the shoulder, the standard ice mixture gives an excellent fit to the 3.38 – 3.64 μm spectrum of GL 2136.

The laboratory fit shown in Fig. 5 corresponds to column densities of 3.1 x 10^{17} cm^{-2} for solid H_2CO and 2.0 x 10^{17} cm^{-2} for solid CH_3OH. With an H_2O column density of 5.0 x 10^{18} cm^{-2} (Table 2) we then find average abundances relative to solid H_2O of 6.2 % and 4.0 % for H_2CO and CH_3OH, respectively. The feature depths were constrained by the shape of the residual obtained after subtraction from the GL 2136 spectrum. The criteria used were that, first, the slope of the spectrum longward of 3.56 μm should decrease monotonically with wavelength, and, second, that the 3.54 and 3.47 μm features are properly subtracted out. Thus we find uncertainties in the column densities of 25 % for CH_3OH and 35 % for H_2CO. Due to the uncertain band intensity, the total error in the H_2CO column density as quoted in table 2 amounts to 43 % (see Sect. 4).

The methanol column density deduced from the 3.54 μm feature is about 2 times smaller than that found from the 9.75 μm band (Skinner et al. 1992; Table 2). Similar discrepancies were earlier found for the solid water column densities deduced from the 3 and 6.0 μm features in various sources (Allamandola et al. 1992). This effect may be related to differences in the lines of sight traced at different wavelengths related to scattering effects (Pendleton et al. 1990; Skinner et al. 1992).

Generally, fitting just one absorption feature can only provide a tentative identification due to the possibility of a chance coincidence. In particular, the observed 3.47 μm feature falls close to the position of the symmetric stretching modes of the organic $-CH_2-$ and $-CH_3$ groups, either in aliphatic molecules or as sidegroups on aromatic structures (d'Hendecourt & Allamandola 1986; Schutte et al. 1990; Sandford et al. 1991). In this view, the depressions near 3.38 and 3.41 μm in the GL 2136 spectrum could be interpreted as indications of the $-CH_3$ and $-CH_2-$ asymmetric stretching modes, further adding to the ambiguity of an identification based on the 3.36 – 3.66 μm region only. However, additional support for the proposed identification of the 3.47 μm feature with solid H_2CO may be obtained from previous low-resolution KAO spectroscopy in the 5 – 8 μm region (Tielens & Allamandola 1987b; Fig. 7). It has been noticed that the position and shape of the 6.0 and 6.8 μm absorption bands toward GL 2136 could be indicative of the presence of the ν_2 5.8 and ν_3 6.7 μm features of solid H_2CO (Schutte 1988). For the solid formaldehyde column density inferred from the 3.47 μm band (Table 2), the 5.8 and 6.7 μm features should have op-

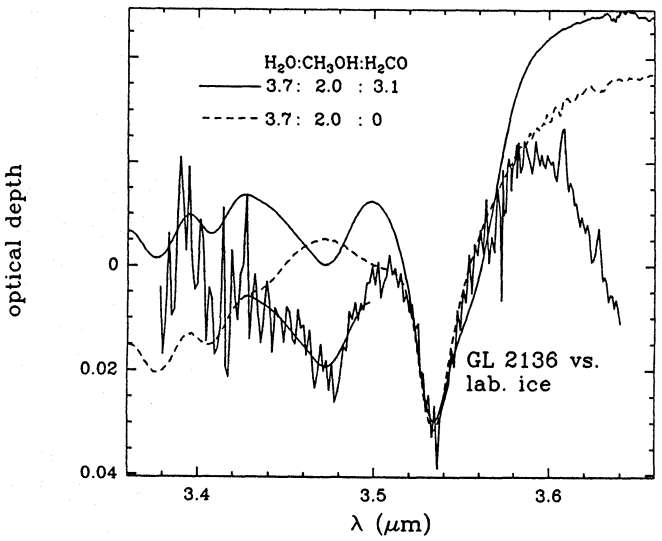

Fig. 5. The GL 2136 optical depth plot compared to the laboratory spectra of the ice mixtures $H_2O/CH_3OH/H_2CO$ = 3.7:2.0:3.1 (the "standard mixture"; solid curve) and 3.7:2.0:0 (dashed curve). The laboratory spectra have been temperature averaged at a ratio 50K:70K:100K = 2:4:1. Part of the spectrum of the standard mixture is shown again overlaying the observed 3.47 μm feature

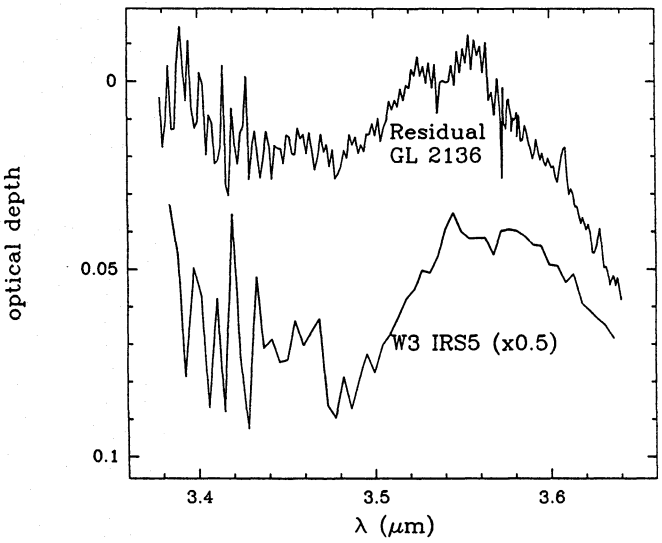

Fig. 6. Residual obtained after subtracting the spectrum of the standard ice mixture from the optical depth plot of GL 2136 (Fig. 5). For comparison, the optical depth plot of W3 IRS5, obtained by the same baseline subtraction procedure used for the optical depth plot of GL 2136 (Fig. 3), is also shown. The spectrum of this object shows no sign of solid methanol or formaldehyde features. For clarity, the W3 IRS5 spectrum was multiplied by 0.5 and shifted 0.06 units downward. The W3 IRS5 data were obtained from Allamandola et al. 1992

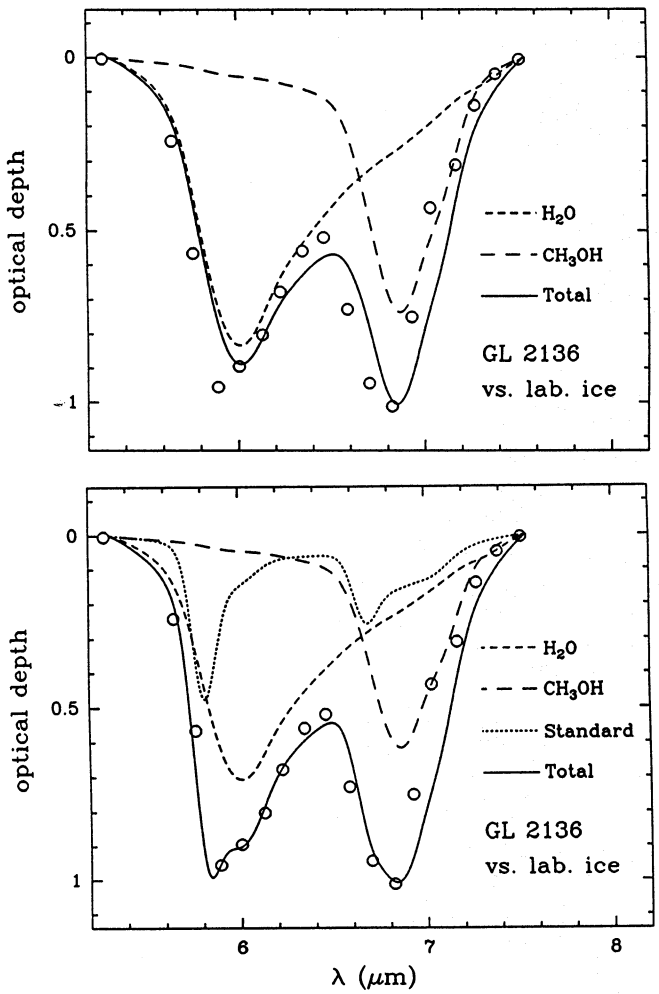

Fig. 7. Low resolution 5 – 8 μm KAO spectrum ($\lambda/\Delta\lambda \approx 50$) of GL 2136 (from Tielens and Allamandola 1987b). In the top figure, a comparison is made to a composite spectrum (solid line) of solid H_2O (short dashed line) and solid CH_3OH (long dashed line). In the bottom figure a comparison is made to a composite spectrum (solid line) of solid H_2O (short dashed line), solid CH_3OH (long dashed line), and the standard ice mixture (very short dashed line). The spectrum of the standard mixture is dominated by the two strong H_2CO features at 5.8 and 6.7 μm. All spectra were temperature averaged at a ratio 50K:70K:100K=2:4:1, except for CH_3OH, for which the spectrum obtained directly after deposition at 10 K was used

tical depths of ~ 0.14 and 0.07, respectively. To test whether the presence of features of such intensity is consistent with the KAO spectrum, Fig. 7 presents two different laboratory fits. The first fit was produced by adding the temperature–averaged 6.0 μm feature of pure H_2O ice to the 6.8 μm band of pure CH_3OH ice at 10 K. The 6.8 μm band of pure amorphous methanol ice was found to be a good template of the interstellar feature (Tielens and Allamandola 1987b, Tielens 1989). We want to emphasize however that it seems highly unlikely that methanol is the only carrier of this feature, because it is found for various sources that the amount required to produce this feature is much larger than the quantities indicated by other methanol features (e.g.; Grim et al. 1991, Skinner et al. 1992, Schutte et al. 1991). For example, in the case of GL 2136, the ratio of the 6.8 to 6.0 μm features would indicate $[CH_3OH]/[H_2O] \approx 0.8$, an order of magnitude larger than found from the 3.54 and 9.75 μm features (Table 2). Since we consider the methanol band only as a template for the interstellar 6.8 μm absorption, we did not take a temperature average in this case. For the second fit we combined the methanol and water spectra with the temperature averaged spectrum of the standard mixture. This spectrum is dominated by the ν_2 5.8 and ν_3 6.7 μm formaldehyde bands. For both the 2 component and 3 component fit, the relative magnitudes of the component spectra were varied freely until an optimum match was achieved. Like the interstellar data, all model spectra were normalized to 0 at 5.28 and 7.52 μm and smoothed to a resolution of 0.13 μm. It can be seen that adding the standard mixture significantly improves the fit to the GL 2136 spectrum in both regions where formaldehyde features are present. The successful fit of the 5 – 8 μm spectra with the composite laboratory spectrum including the H_2CO features supports the assignment of the 3.47 μm feature to solid formaldehyde. The fit as displayed in Fig. 7b corresponds to a solid formaldehyde abundance of 9.6 ± 2 % of solid H_2O, consistent with the amount deduced from the 3.47 μm feature.

In summary, the presence of solid formaldehyde toward GL 2136 is indicated both by the presence of the 3.47 μm band in the new UKIRT data and by the previous low resolution KAO spectroscopy in the 5 – 8 μm region. The H_2CO abundance equals 6.2 ± 2.7 % of solid H_2O, comparable to the amount of solid CO and CH_3OH observed toward this source (Table 2).

4. Infrared spectroscopy of formaldehyde containing ices

Previous laboratory studies have shown that the position of the ν_5 band of solid formaldehyde depends sensitively on the composition of the ice matrix (van der Zwet et al. 1985). For this reason, comparing the 3.47 μm interstellar feature to spectroscopy of various ices could yield important information on the composition of the formaldehyde–containing ices toward GL 2136. Further constraints are provided by the 3.54 and 9.75 μm features.

Our general experimental procedures for preparing astrophysical ice analogs have been outlined previously (Gerakines et al. 1995, and references therein). As a consequence of special storage requirements, the reactive formaldehyde must be deposited separately from the other sample constituents through an independent deposition system (Schutte et al. 1993). Due to the independent deposition, the actual abundance of formaldehyde in the ice samples, deduced from the intensities of the IR features, could vary by up to 20 % from the intended composition. Spectra of the ice samples were obtained with a BioRad FTS 40A spectrometer equipped with globar source, KBr beamsplitter and DTGS detector at a resolution of 1 cm^{-1}. To monitor the temperature dependence the ices were, after deposition at 10 K, subjected to gradual warm-up (~ 2 K $min.^{-1}$), and spectra were taken at regular intervals. Before scanning a spectrum, the substrate temperature was kept constant for 5 minutes to allow equilibration.

Table 3. Summary of the experimental results

no.	Mixture					ν_5 H_2CO (f.1)			ν_1 H_2CO + ν_3 CH_3OH (f.2)		
	H_2O	CH_3OH	H_2CO	CO	T K	ν cm^{-1}	FWHM cm^{-1}	A cm/molec.	ν cm^{-1}	FWHM cm^{-1}	A[1] cm/molec.
1			1		ave	2884.4	23	2.7(-18)	2822.1	28	3.7(-18)
					10	2884.0	23		2821.8	28	
					70	2884.5	23		2822.0	28	
					100	2884.8	22		2823.3	28	
2		1			ave				2828.5	29	6.6(-18)
					10				2828.2	31	
					70				2828.4	29	
					100				2829.3	28	
3		1.8	3.0		ave	2881.0	21	2.0(-18)	2821.0	36	4.8(-18)
					10	2880.7	22		2822.0	36	
					70	2881.0	21		2820.5	36	
					100	2881.0	21		2821.1	36	
4		2.3	3.0		ave	2880.4	20		2825.0	38	
					10	2879.9	21		2825.3	38	
					70	2880.3	20		2824.8	38	
					100	2882.0	19		2828.5	35	
5	3.6		3.0		ave	2886.9	34	2.3(-18)	2828.4	45	4.0(-18)
					10	2888.9	35		2830.8	43	
					70	2886.8	35		2828.7	45	
					100	2885.2	31		2824.3	45	
6	66		3.0		ave	2889.2	27		2825.6	42	
					10	2890.9	25		2828.3	41	
					70	2889.3	26		2825.6	42	
					100	2887.6	40[2]		2823.0	48[2]	

Table 3 lists the positions and widths of the ν_5 feature of H_2CO (henceforth feature 1) and the combined ν_1 H_2CO and ν_3 CH_3OH features (henceforth feature 2) in a number of ice mixtures. The composition was obtained from the intensities of the ν_2 H_2CO mode near 1720 cm^{-1}, the ν_8 CH_3OH mode near 1030 cm^{-1}, the CO stretching mode near 2140 cm^{-1}, and the H_2O librational mode near 770 cm^{-1}, with band strengths of 9.6 x 10^{-18} cm, 1.8 x 10^{-17} cm, 1.1 x 10^{-17} and 3.0 x 10^{-17} cm, respectively (d'Hendecourt & Allamandola 1986; Schutte et al. 1993; Gerakines et al. 1995). Fig. 8 displays the (temperature averaged) 3000 to 2720 cm^{-1} (3.333 – 3.676 μm) spectra for most of these mixtures. It can be seen that when H_2CO is included feature 2 is generally broader and in some cases displays a weak red shoulder, apparently caused by the ν_1 H_2CO mode merging with the ν_3 CH_3OH feature. Besides the primary bands, the methanol–containing ices show additional structure at the high frequency end of the spectrum. In particular if H_2O is present two shallow features appear at 2961 and 2934 cm^{-1} (3.377 and 3.408 μm).

The position of feature 1 and 2 depends sensitively on the overall ice composition. A casual inspection of Table 3 shows that the position of feature 1 is especially sensitive to the H_2CO/CH_3OH ratio (cf.; Mix. 3 and 4; 6, 9 and 10; 13 and 14), but is rather insensitive to the H_2O abundance (cf.; Mix. 3, 10, and 13; 8, 9, and 14) unless an H_2O overabundance is applied (Mixture 15). On the other hand the position and width of feature 2 depends strongly on the CH_3OH/H_2O ratio (cf.; Mix. 3, 10, and 13; 8, 9, and 14), but also on the H_2CO/CH_3OH ratio (cf.; Mix. 6, 9, and 10; 3 and 4; 13 and 14).

In general, for pure and diluted solid formaldehyde the ν_1 and ν_5 C–H stretching modes are strongly blue shifted from their gas phase positions at 2766 and 2843 cm^{-1}, respectively (Blau & Nielsen 1957; van der Zwet et al. 1985). The positively charged part of polar or polarizable species can draw electrons away from the formaldehyde CO bond, thus weakening the repulsion between the CO and CH bond of the formaldehyde, resulting in a stronger CH bond with a higher vibrational frequency (Schneider & Bernstein 1956). For H_2O–H_2CO the blue shift is quite large. The H_2O molecules are able to form a hydrogen bond with the formaldehyde, resulting in a significant transfer of charge to the H atoms of the water (Nelander 1980; Fukunaga & Morokuma 1993). On the other hand, pure H_2CO ice does not form H–bonds. Instead neighboring molecules interact through the positively charged C and negatively charged O atom. Because this is a weaker interaction, the C-H stretching modes are less blue shifted in this case (Schneider & Bernstein 1956). A similar situation occurs for the $H_2S.H_2CO$ complex, where the C...S interaction dominates (Nelander 1978). Likewise, the blue shift of the ν_1 and ν_5 features is relatively small for H_2CO mixed in CH_3OH (Table 3), indicating that the interaction takes place between the formaldehyde O and methanol C rather than through H–bonding. It is interesting to note that

Table 3. (continued)

no.	Mixture				T	ν_5 H_2CO (f.1)			ν_1 H_2CO + ν_3 CH_3OH (f.2)		
	H_2O	CH_3OH	H_2CO	CO	K	ν cm^{-1}	FWHM cm^{-1}	A cm/molec.	ν cm^{-1}	FWHM cm^{-1}	A[1] cm/molec.
7	3.7	2.0			ave				2829.9	25	8.3(-18)
					10				2830.1	25	
					70				2829.9	25	
					100				2830.2	26	
8	1.9	1.0	3.2		ave	2882.7	26		2826.2	36	
					10	2883.1	27		2828.1	37	
					70	2882.4	26		2826.0	36	
					100	2883.0	25		2825.1	35	
9	3.8	1.0	3.0		ave	2882.4	33		2829.8	36	
					10	2884.2	34		2830.1	35	
					70	2882.2	33		2829.9	36	
					100	2882.3	29		2829.3	38	
10	3.7	2.0	3.1		ave	2879.8	28	1.1(-18)	2829.4	35	4.0(-18)
					10	2882.1	31		2829.9	35	
					70	2879.5	28		2829.4	35	
					100	2880.1	26		2829.4	37	
11	3.7	2.0	3.5		ave	2880.8	27		2829.1	36	
					10	2882.0	29		2829.7	35	
					70	2880.3	27		2829.0	35	
					100	2880.8	23		2828.5	38	
12	3.7	2.0	3.5	1.3	ave	2882.4	28		2830.3	35	
					10	2886.1	32		2830.8	35	
					70	2881.9	28		2830.4	34	
					100	2882.1	23		2829.0	36	
13	7.6	1.0	3.1		ave	2883.5	39		2830.7	35	
					10	2889.8	36		2831.1	33	
					70	2887.1	39		2830.7	33	
					100	2878.9	37		2830.5	39	
14	7.6	2.0	3.3		ave	2879.9	36	9.0(-19)	2830.3	33	3.6(-18)
					10	2888.2	37		2831.0	32	
					70	2878.6	36		2830.3	33	
					100	2879.0	32		2830.2	36	
15	11	2.0	2.9		ave	2871.0	20		2831.0	31	
					10	–	–		2831.4	29	
					70	2869.7	–		2831.0	31	
					100	2872.0	19		2830.8	35	
16[3]	3.7	2.2	1.5	0.34	ave	2879.3	–		2830.4	32	
					10	2881.0	–		2830.2	33	
					70	2878.5	–		2830.5	32	
					100	2879.0	–		2830.5	33	
GL 2136						2878.7±1.5	25		2828.6±1.0	35	

[1]Band strength obtained by integrating the optical depth and deviding by the combined column density of methanol *plus* formaldehyde. [2]Combined FWHM of the double peak. [3]Obtained by irradiation of $H_2O/CH_3OH/H_2CO$ = 3.7:2.0:3.1 at dose R = 0.36.

adding modest quantities of H_2O does not lead to an appreciable blue shift of the ν_5 feature. Apparently the presence of the CH_3OH in some way prevents H_2CO from forming hydrogen bonds with H_2O, but the mechanism involved in this process is unclear.

5. Composition of the formaldehyde–containing ices toward GL 2136

The precise wavelength of the 3.47 μm feature in GL 2136 appears best fitted by mixtures having $[H_2CO]/[CH_3OH] \approx 1.5$. With less methanol, feature 1 shifts too far to the blue (Table 3, Fig. 8). Furthermore, to obtain a good fit of the 3.54 μm band, the ice mixture needs to contain H_2O, otherwise feature 2 lies

too far to the blue and becomes too broad. The standard mixture (Mixture 10 in Table 3), containing similar abundances of H_2O and H_2CO, produces a good fit of the feature. The presence of H_2O mixed in the H_2CO and CH_3OH ice is furthermore born out by the shallow structure near the short wavelength end of the GL 2136 spectrum (Fig. 5). Corresponding features at 3.377 and 3.408 μm (2961 and 2934 cm^{-1}) only show up in ices containing H_2O (Fig. 5, Fig. 8). Mixture 13 in Table 3 with a two times higher H_2O abundance than standard, also matches the position of the 3.47 μm band, but the match of the 3.54 μm feature is somewhat less favorable in this case. Using an even higher water abundance results in a very poor match for both the 3.47 and 3.54 μm features of GL 2136 (Mixture 15).

An additional constraint on the ice composition is provided by the 8.9 μm and 9.75 μm features of solid methanol which were previously observed toward GL 2136 (Skinner et al. 1992). Fig. 9 compares these bands to the ν_7/ν_{11} and the ν_8 methanol features, respectively, in the mixtures $H_2O/CH_3OH/H_2CO$ = 0/2.0/3.4, 3.7/2.0/3.1 (the standard mixture), and 7.6/2.0/3.3. The ν_8 feature is especially sensitive to the H_2O/CH_3OH ratio (Schutte et al. 1991; Skinner et al. 1992). An excellent fit to the 9.75 μm band is given by the mixture without water, but the fit becomes less favorable with increasing H_2O abundance. On the other hand, the observed ratio of the 8.9 and 9.75 μm features is better reproduced by the water–rich ices. It must be noted that some error in the shape of the 9.75 μm feature may have been introduced by the data reduction which involved the subtraction of the very strong silicate feature on which the methanol band is superimposed (Skinner et al. 1992). It may therefore be tentatively concluded that the standard mixture gives a good overall fit to the 8.5 – 10.5 μm as well as the 3.36 – 3.64 μm and 5 – 8 μm regions toward GL 2136, but that mixtures with significantly higher or lower H_2O content are less successful. Thus, for the formaldehyde–containing ice we estimate $\frac{([H_2CO]+[CH_3OH])}{[H_2O]} \approx 0.7 - 1.8$.

Comparing experiments 11 and 12 it can be seen that adding some CO to the standard mixture induces a significant blue–shift for feature 1 as well as 2, away from the position of the GL 2136 features. It appears that CO is probably not an important constituent of the ices which contain the formaldehyde. The profile of the CO band itself does not provide additional information on its whereabouts, since the CO feature of mixture 12 falls at 2136.6 cm^{-1}, and can provide a fit to the observed band of GL 2136 of similar quality as CO diluted in an otherwise pure H_2O ice (Tielens et al. 1991).

Table 3 lists the band strengths for the most relevant mixtures. These were calibrated relative to the measured intensity of the ν_2 formaldehyde feature near 5.8 μm and the ν_8 methanol feature near 9.75 μm, assuming mixture–independent band strengths of 9.6 x 10^{-18} cm $molec^{-1}$ and 1.8 x 10^{-17} cm $molec^{-1}$, respectively. Due to the independent deposition of the H_2CO , the column density of the H_2CO in the various ice samples could be held constant, allowing us to verify that the former assumption is correct within 10 %. Examples of the baselines used in deriving these band strengths are shown in Fig. 8 for the spectrum of the standard mixture. A strong drop in the intensity of the ν_5 H_2CO feature occurs when both CH_3OH and H_2O are present in the ice mixture (cf., Mix. 3, 10, and 14).

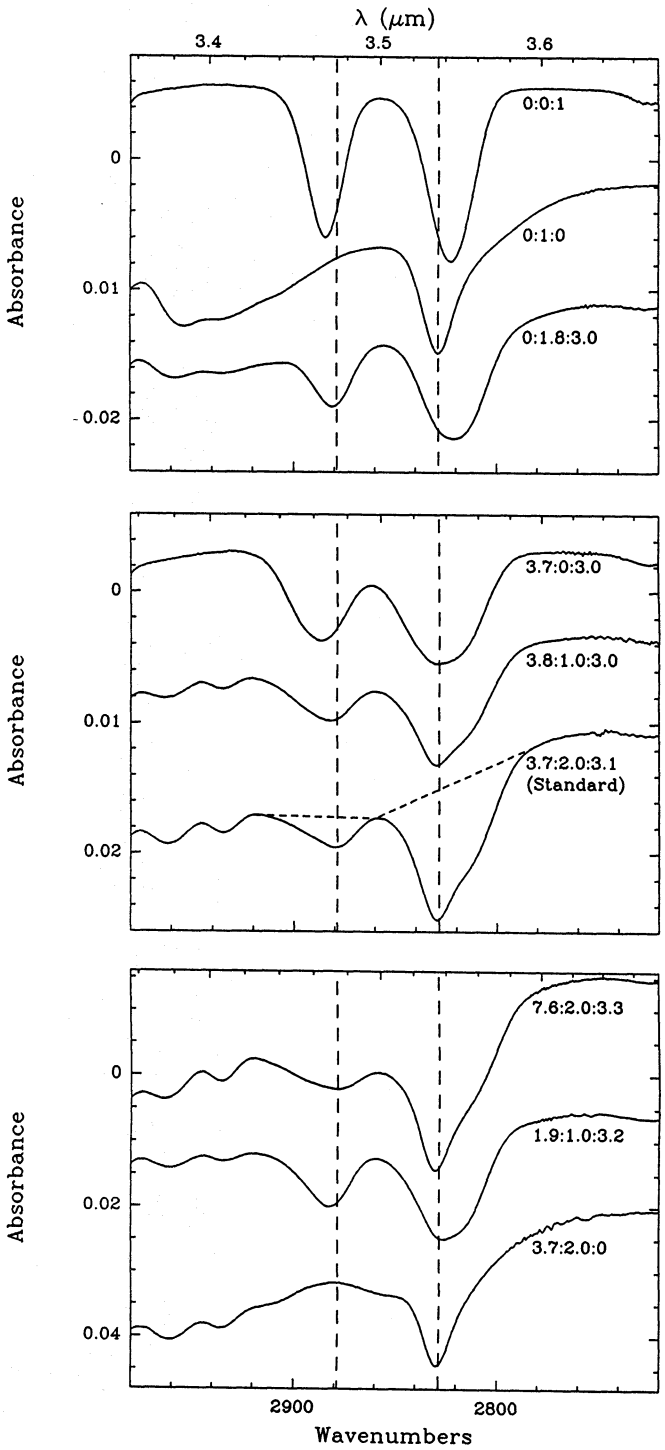

Fig. 8. Summary of spectra of the laboratory ice samples. For each curve, the corresponding H_2O:CH_3OH:H_2CO ice ratio is indicated on the right hand side. All spectra are temperature averages at a ratio 50K:70K:100K=2:4:1. The vertical dashed lines give the positions of the observed GL 2136 features. As an example, short dashed lines give for the standard mixture the baselines used in deriving the band intensities of Table 3

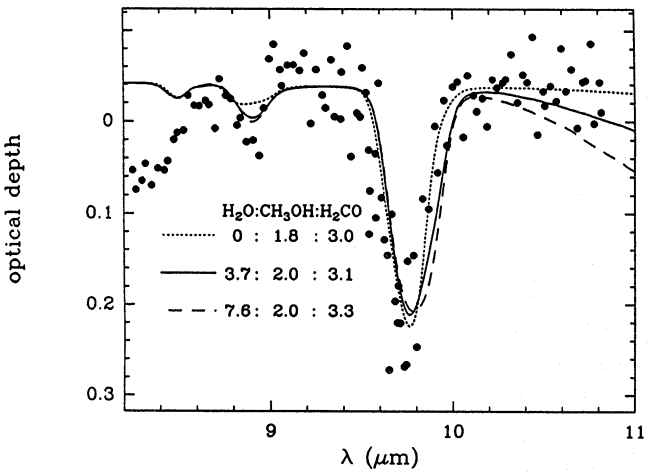

Fig. 9. Comparison of the 8 – 11 μm spectrum of GL 2136 including the narrow 8.9 and 9.75 μm absorption features of solid methanol (from Skinner et al. 1992) with the spectra of a number of laboratory ices; H_2O:CH_3OH:H_2CO = 0:1.8:3.0 (short dashed line), 3.7:2.0:3.1 (the standard mixture; solid line), and 7.6:2.0:3.3 (long dashed line). The GL 2136 spectrum was obtained by subtracting the strong 9.7 μm interstellar silicate feature (Skinner et al. 1992)

This decrease may be related to the presence of some structure near the position of this band in mixtures of H_2O and CH_3OH, which may cancel out part of this feature (Fig. 8). The variation in the band intensity introduces ~ 20 % uncertainty in the H_2CO column density derived from the 3.47 μm band. The variation of the strength of the combined ν_1 H_2CO/ν_3 CH_3OH feature is primarily related to the variation in the relative contribution of the methanol and formaldehyde bands and does not produce any significant uncertainty in the CH_3OH column density determined from the 3.54 μm feature of GL 2136.

In summary comparison of the GL 2136 data to the laboratory spectra reveals a number of properties of the ice mantles. An overview is given in Table 4. First, the position of the 3.47 μm feature requires $[H_2CO]/[CH_3OH] \approx 1.5$. Because this ratio is equal to the ratio of the column densities (Table 2), it appears that the solid formaldehyde and methanol toward GL 2136 are intimately mixed. Second, a considerable amount of H_2O has to be mixed with the methanol and formaldehyde ice in order to fit the 3.54 μm feature. However, fits of the 9.75 μm and 3.54 μm features are poor when the H_2O abundance greatly exceeds the abundance of H_2CO plus CH_3OH. Thus, the formaldehyde containing ices seem to be dominated by the two hydrogenated forms of CO, i.e., CH_3OH and H_2CO. From the restriction on the H_2O quantity that can be mixed in this ice component it follows that most (i.e., $\gtrsim 90$ %) of the water resides in a separate phase consisting of almost pure H_2O ice with probably some CO.

The total gas phase column density toward GL 2136 is estimated to be $N_H \approx 1.8 \times 10^{23}$ cm^{-2} from the optical depth of the 10 μm silicate feature. Thus the overall abundances abundances of solid H_2CO and CH_3OH are of order $\sim 10^{-6}$, significantly higher than found in the gas phase in general molecular clouds (van Dishoeck et al. 1993).

Table 4. Phases of the ice mantles toward GL 2136

Type	Approximate composition	Abundance by mass
I	H_2O:CO=100:4	0.75
II	H_2O:CH_3OH:H_2CO=4:2:3	0.25

6. Discussion

6.1. Origin of solid formaldehyde and methanol

Because production of formaldehyde and methanol by pure gas–phase chemistry is an inefficient process (Millar et al. 1991; Chièze et al. 1991, Shalabiea & Greenberg 1994), the production needs to take place on the grains themselves in order to account for the high abundances toward GL 2136. Two mechanisms have been proposed. First, solid formaldehyde may be produced by grain surface hydrogenation upon CO accretion (Tielens & Hagen 1982; Hasegawa et al. 1992; Caselli et al. 1993):

$$CO + H \rightarrow HCO \quad (1)$$

$$HCO + H \rightarrow H_2CO \quad (2)$$

Likewise the formation of methanol could proceed by hydrogenation of CO, either with formaldehyde or the unstable isomer HOCH as an intermediate (Hasegawa et al. 1992):

$$CO + 2H \rightarrow HCOH \quad (3)$$

$$HCOH + 2H \rightarrow CH_3OH \quad (4)$$

$$H_2CO + 2H \rightarrow CH_3OH \quad (5)$$

Recent studies of the reaction of CO with impinging H atoms question the viability of reactions 2 and 3 (Hiraoka et al. 1994). Although H_2CO and CH_3OH were produced, the conversion was found to be quite low, indicating a low efficiency for reaction 2 and 3. Unfortunately, no quantitative information could be derived from these experiments, so that any model results are still uncertain. Still, the ability of surface chemistry to generate considerable quantities of H_2CO and CH_3OH on interstellar grain mantles appears questionable and further experiments are warranted.

Second, formaldehyde and methanol could be formed by ultraviolet photolysis. In this context, the reaction scheme

$$H_2O + h\nu \rightarrow OH + H \quad (6)$$

$$CO + 2H \rightarrow H_2CO \quad (7)$$

was proposed (Shalabiea & Greenberg 1994). If CH_3OH is initially present in the grain mantles, another reaction path could be (Allamandola et al. 1988; Gerakines et al. 1996):

$$CH_3OH + h\nu \rightarrow H_2CO + H_2 \quad (8)$$

Ultraviolet photolysis of formaldehyde may lead to the formation of methanol through two independent pathways. First, two formaldehyde molecules may photo–associate (Sodeau & Lee 1978):

$$H_2CO + H_2CO \rightarrow CH_3OH + CO \quad (9)$$

In the presence of a photochemical source of atomic hydrogen methanol may form by hydrogen addition:

$$H_2CO + 2H \rightarrow CH_3OH \quad (10)$$

Ultraviolet radiation inside a dense cloud could originate from internal sources such as cosmic ray induced photons and the protostar itself and from the penetration of the diffuse galactic field (e.g., Greenberg 1973; Sternberg et al. 1987; Rawlings 1993; Prasad & Tarafdar 1983; Schutte & Greenberg 1991, and references therein). The cosmic ray produced internal ultraviolet flux amounts to $\sim 10^3$ photons cm^{-2} s^{-1} ($E_{photon} > 6.2$ eV) for a typical cosmic ray ionization rate of $\xi \approx 10^{-17}$ s^{-1} (Sternberg et al. 1987). The intensity of the penetrating ultraviolet field depends on the position in the cloud as well as the cloud morphology. With an ultraviolet intensity of $\sim 8 \times 10^7$ photons cm^{-2} s^{-1} ($E_{photon} > 6$ eV; Mathis et al. 1983) in the diffuse medium it will be the dominant source in the outer cloud regions. To facilitate comparison of the expected processing of interstellar ices with the results of simulation experiments, we adopt as a convenient measure of the dose the irradiation ratio R, defined as the amount of ultraviolet photons absorbed per solid H_2O molecule, calculated with an average absorption cross section of 2×10^{-18} cm^2 ($E_{photon} > 6$ eV; Okabe 1978). For illustration, with a cosmic ray induced ultraviolet flux of $\sim$ 1000 cm^{-2} s^{-1}, the dose equals R = 0.06 after 10^6 years. Of course, the dose could be much higher even with a relatively short stay in a region where the interstellar field penetrates, or in the neighbourhood of a protostellar object.

To assess the viability of formaldehyde production by ultraviolet photolysis through reaction 6 and 7, we briefly summarize the available experimental results. Zhao (1990) studied the photolysis of mixtures of CO in an overabundance of H_2O. It was found that after a dose of R $\approx$ 5, about 2.6 % of the originally deposited CO was converted to H_2CO, while the main product of the photolysis was CO_2. Adding a limited quantity of CH_4, an efficient source of atomic H under ultraviolet irradiation, increased the H_2CO yield to 3.8 %. Schutte (1988) found in similar H_2O/CO mixtures a H_2CO yield of 4.3 % of the deposited CO after a dose of R $\approx$ 0.9. These results indicate that reactions 6 and 7 maximally convert a few percent of the CO to H_2CO. The apparent saturation of the formaldehyde growth with dose for R $\gtrsim$ 1 indicates that destruction and production reach a balance. It follows that, adopting a maximum conversion of 5 %, a CO quantity of $\sim$ 1.4 times the solid water abundance should have been present at the time when the photochemical production took place in order to produce the $\sim$ 7 % H_2CO in the ice mantles toward GL 2136. The maximum observed CO abundance in interstellar ices is 20 – 40 % of H_2O (Tielens et al. 1991; Chiar et al. 1994), it appears unlikely that such a quantity could have been present during the evolution of the icy mantles, although perhaps at some phase during the collapse phase of the pre–stellar cloud CO may have been largely depleted on the grains. Perhaps it is possible that under some conditions not yet covered by experimental simulations the photochemical production of H_2CO from CO could be more efficient, e.g., at the relatively high temperatures in the protostellar environment, or perhaps in the presence of large quantities of H_2 in the ice mantles (Sandford & Allamandola 1993b; Buch & Devlin 1994; Dissly et al. 1994).

Alternatively, formaldehyde may be produced photochemically from solid CH_3OH. However, for pure methanol ice, it is found that at most $\sim$ 8 % of the methanol in the original sample converts to H_2CO at any dose (Gerakines et al. 1996), far less than necessary to account for the H_2CO abundance relative to CH_3OH toward GL 2136.

A comparison of the composition of the ices toward GL 2136 and toward W33 A and NGC7538 IRS9 also appears to argue against a photochemical origin of solid formaldehyde. Both W33 A and NGC7538 IRS9 show a feature at 4.62 μm, which has been associated with a -CN bearing species ("XCN") and which is probably produced by energetic processing (Lacy et al. 1984; Tegler et al. 1995). In particular, ultraviolet photolysis of ices containing H_2O, CO, and NH_3 produces a feature that matches the interstellar structure very well. This band has been assigned to the OCN^- ion (Grim & Greenberg 1987). The depth of the 4.62 μm feature relative to the 3 μm water band equals $\frac{\tau(4.62\mu m)}{\tau(3\mu m)} = 0.13$ and 0.05 for W33 A and NGC7538 IRS9, respectively (using $\tau(3\mu m) = 10$ toward W33 A; Schutte 1996), indicating a substantial amount of photoprocessing toward these objects (i.e., R $\gtrsim$ 1; Schutte 1988; 1996). NGC7538 IRS 9 and W33 A furthermore show the 3.54 μm feature, indicating column densities of solid methanol close to 10 % of H_2O (Grim et al. 1991; Allamandola et al. 1992; Schutte 1996). Additionally, while the solid CO abundance toward W33 A is somewhat lower that toward GL 2136, the amount of solid CO toward NGC 7538 IRS9 is as high as 10 % of H_2O (Tielens 1991). In spite of the presence of the potential H_2CO precursors and the high degree of energetic processing, no feature at 3.47 μm or any sign of the 5.8 and 6.7 μm H_2CO features are found toward W33 A and NGC7538 IRS9 (Allamandola et al. 1992; Tielens

& Allamandola 1987b; Tielens 1989). The absence of the latter bands gives strict upper limits to the formaldehyde abundance of less than $\sim$ 1 % of H_2O. In contrast, the 4.62 μm feature was not observed toward GL 2136, yielding an upper limit of $\frac{\tau(4.62\mu m)}{\tau(3\mu m)} \leq 0.025$ (Geballe 1986a; b). Thus the observations indicate a negative rather than a positive correlation between the degree of photoprocessing of the mantles and the occurrence of solid H_2CO; i.e., it appears that solid formaldehyde is destroyed rather than formed by ultraviolet irradiation. Indeed, in an experiment involving the irradiation of the standard mixture ($H_2O/CH_3OH/H_2CO$ = 3.7/2.0/3.1), half of the formaldehyde is destroyed after a dose of R = 0.3. Thus for example toward W33 A, where the ices appear to have been ultraviolet processed at a dose in excess of R = 1, it is expected that less than $\sim$ 10 % of any accreting formaldehyde could have survived. In contrast, methanol was not significantly destroyed by the irradiation, i.e., more than 95 % survived at R = 0.3. Thus ultraviolet processing of interstellar ices efficiently destroys H_2CO that is *initially* present.

To study the efficiency of the photochemical formation of methanol from formaldehyde, we irradiated an ice mixture H_2O:NH_3:H_2:H_2CO = 100:3:15:15. The 3 admixed species produce atomic hydrogen under ultraviolet photolysis (e.g., d'Hendecourt et al. 1986) and thus should promote CH_3OH production through reaction (10). It was found that the photochemical conversion of formaldehyde to methanol was quite inefficient, i.e., for each formaldehyde molecule lost as a result of the photolysis only 0.06 molecule of methanol was formed. Likewise, photolysis of pure formaldehyde, in which process (7) should proceed with optimum efficiency, yields only minor quantities of CH_3OH (Gerakines et al. 1996). Thus, a photochemical origin of the large quantities of solid methanol observed toward GL 2136 and other embedded protostellar sources appears to be excluded.

In summary, both mechanisms that have been proposed for the production of large quantities of solid methanol and formaldehyde on icy grain mantles appear to face serious problems; i.e., experimental results indicate that both the surface hydrogenation and mantle photoprocessing fall short of producing the high abundances of methanol and formaldehyde found toward GL 2136. Further studies under a wider range of conditions, e.g., in the presence of solid H_2, are necessary to explore the possibility of photochemical production of formaldehyde. Also, the temperature dependence of the CO hydrogenation is still unexplored, especially the temperature of the atomic hydrogen gas. The inefficiency indicated by the experimental results contrasts with the observed high deuteration of interstellar formaldehyde, which is thought to imply that grain surface hydrogenation plays an important role in the H_2CO formation, at least in Orion (Turner 1990). One may speculate that perhaps H_2CO and CH_3OH formation took place during a period where the icy mantles were exposed to a high flux of atomic hydrogen and deuterium. In this scenario the high incidence of H–atoms would compensate for the indicated low efficiency of reactions 2 and 3. In this context it must be noted that CO hydrogenation is not necessary restricted to the grain surface, but may also take place inside the mantle, since it was found that hydrogen atoms are able to penetrate and diffuse through molecular ice at temperatures as low as 10 K (Hiraoka et al. 1995).

6.2. *Implications for the chemical conditions in dense clouds*

The discovery of solid formaldehyde toward GL 2136 confirms earlier indications of the presence of formaldehyde in icy mantles deduced from the observed excess of gaseous formaldehyde in hot core sources (Blake et al. 1987; Turner 1990). It strongly supports models of dense cloud chemistry which use H_2CO production on and desorption from grains to reproduce the observed gas abundances (Federman & Allen 1991, Shalabiea & Greenberg 1994). Indeed, toward GL 2136, it is found that also gas phase H_2CO is enhanced relative to CH_3OH, compared to W33 A and NGC 7538 IRS9 (van Dishoeck et al, in preperation).

From spectroscopic arguments it was derived that the ice toward GL 2136 consists of two distinct phases; i.e., one dominated by solid H_2O (henceforth "type I" ice) and one with solid H_2CO, CH_3OH and H_2O in similar abundances (henceforth "type II" ice). Earlier observations of solid CO at 4.68 μm have shown that ices dominated by apolar species (CO, O_2, N_2) exist in dense clouds (Sandford et al. 1988; Tielens 1991; henceforth "type III" ice). Two explanations have been put forward to account for the existence of these distinct phases. In the first model, each phase may reflect the gas phase chemical conditions at the time of accretion (Sandford et al. 1988; Tielens 1991). In this model, type III ice is formed in the most dense and obscure cloud regions where virtually no atomic H and O are present in the gas phase and molecules like CO and O_2 condense without further surface alteration. The H_2O–rich ices are produced in more tenuous and translucent outer cloud regions, where atomic hydrogen and oxygen are abundant and accreting O and O_2 are hydrogenated on the grain surfaces to produce H_2O. In the second model, an initially homogeneously condensed ice mixture is differentiated by a selective desorption mechanism (Schutte & Greenberg 1991). Desorption of ices in dense clouds are thought to involve impulsive heating of the grain, for example by a cosmic ray particle or by the explosive release of stored chemical energy (Greenberg 1979, d'Hendecourt et al. 1982, Léger et al. 1985) and is probably highly selective with respect to the volatility of the ice components (Schutte & Greenberg 1991, Léger et al. 1985, Hasegawa & Herbst 1993a). Thus H_2O can probably be separated efficiently from highly volatile species like CO, O_2 and N_2 by selective desorption. It seems unlikely that methanol and formaldehyde are separated efficiently from water ice in this way, because, in particular, methanol is probably too refractory to be desorbed efficiently by the impulsive heating events (Schutte & Greenberg 1991, Hasegawa & Herbst 1993a). However, heating near the protostar may result in sublimation of formaldehyde and methanol while the water remains solid (Sandford & Allamandola 1993a). At a later stage type II ice may form when the formaldehyde and methanol recondense on the grain mantles. Alternatively, the type I and II ices observed toward GL 2136 could arise from chemically distinct cloud environments. In this case the ices could correspond to

spatially separated regions along the line of sight, but could also correspond to layers of different ices on individual grains (i.e., an "onion shell" structure). The latter situation would occur when a grain encountered different chemical conditions while in the dense cloud (e.g., Tielens et al. 1991, Schutte 1996).

Owing to the unknown formation mechanism of solid H_2CO and CH_3OH (Sect. 6.1), it is at present far from clear which physical and chemical properties characterized the cloud environment that gave rise to their formation. Future observations of solid formaldehyde and methanol in various cloud environments; i.e., toward background field stars as well as embedded sources, are necessary to study whether such ices are found throughout dense clouds or are restricted to circumstellar regions. Especially, the strong H_2CO 5.8 and 6.7 μm bands, accessible by the Infrared Space Observatory (ISO), could be sensitive tracers of type II ice.

7. Conclusions

We summarize the main conclusions of this paper:

1. Infrared spectroscopy of GL 2136 from 3.38 to 3.77 μm reveals narrow (FWHM $\approx$ 0.04 μm) absorption features at 3.47 μm and 3.54 μm.

2. The 3.54 μm feature has been previously detected toward other embedded protostars and can be assigned to solid CH_3OH. The narrow 3.47 μm feature has not been previously detected. Fits with spectra of laboratory ice analogs suggest an assignment of the new feature to the ν_5 mode of solid H_2CO. A fit of the very low resolution air–borne KAO 5 – 8 μm spectrum of GL 2136 involving the strong 5.8 and 6.7 μm H_2CO features supports this assignment. The derived column densities of H_2CO and CH_3OH are 6.2 $\pm$ 2.7 % and 4.0 $\pm$ 1.0% relative to solid water, respectively.

3. A detailed comparison with spectra of laboratory ice mixtures shows that the H_2CO and CH_3OH ices are probably intimately mixed, together with a considerable amount of H_2O. However, the bulk of the solid H_2O resides in a separate phase of almost pure water ice. Thus we distinguish two different types of ice mantles toward GL 2136: one dominated by solid H_2O (Type I ice), and one rich in solid CH_3OH and H_2CO (Type II ice).

4. Laboratory simulation indicates that the photochemical production of formaldehyde in astrophysical ice analogs is insufficient to produce the observed abundances. Indeed, the apparent anti–correlation between the intensity of the 4.62 μm XCN feature and the abundance of solid H_2CO toward GL 2136, W33 A and NGC7538 IRS9 may indicate that UV processing leads to destruction rather than formation of H_2CO, consistent with the experimental results, which show that solid H_2CO is highly susceptible to photochemical destruction. Also, the efficiency of the reaction of solid CO and atomic H, which could produce H_2CO and CH_3OH on the grain surfaces, appears to be low. The mechanism responsible for producing H_2CO and CH_3OH in interstellar ices still remains unclear.

5. We note that the apparent separation of H_2CO and CH_3OH from water ice in the protostellar cloud toward GL 2136 could relate to the large variation in the abundances of these molecules relative to H_2O observed toward comets (Bockelée-Morvan et al. 1995).

In the near future ISO will produce high quality observations of ice features in spectral windows which are inaccessible from the ground. These new data may be able to clarify some of the issues raised above:

1. To confirm the presence of solid formaldehyde toward GL 2136, high resolution observations of the ν_2 and ν_3 modes near 5.8 and 6.7 μm are necessary. In general, observing these bands toward obscured sources will probe solid formaldehyde much more sensitively than the ν_5 feature near 3.47 μm which, in astrophysically relevant mixtures, has a $\sim$ 10 times lower peak depth than the ν_2 mode. Therefore, such observations may provide important information on the distribution of type II ices throughout dense clouds and in this way shed light on the physical and chemical conditions that gave rise to their origin.

2. Observing ice mantle components produced by energetic processing, e.g., CO_2 (d'Hendecourt et al. 1986), will clarify the possible anti-correlation between the H_2CO abundance and the amount of processing of interstellar ices.

Acknowledgements. We gratefully acknowledge Lou Allamandola and Scott Sandford for providing us with the electronic version of the 3050 – 2650 cm^{-1} spectroscopy toward embedded objects from Allamandola et al. 1992. Likewise, we thank Xander Tielens for providing the electronic version of the 8.2 – 10.8 μm spectrum of GL 2136 from Skinner et al. 1992. We thank Roland Gredel for his assistance with the NTT observations. A special acknowledgement is extended to Menno de Groot for his continuous efforts in keeping the Leiden laboratory in optimal condition. This work was partially funded by NASA grants NGR 33-018-148 and NAGW 4039, and by a PIONIER grant from the Netherlands Organization for Scientific Research (NWO). Support for Willem Schutte from ASTRON and SRON is acknowledged as well. The UKIRT observations were obtained as part of the UKIRT service program.

References

Allamandola L.J., Sandford S.A., Valero G.J., 1988, Icarus 76, 225
Allamandola L.J., Sandford S.A., Tielens A.G.G.M., Herbst T.M., 1992, ApJ 399, 134
Blake G.A., Sutton E.C., Masson C.R., Phillips T.G., 1987, ApJ 315, 621
Blau H.H. Jr., Nielsen H.H., 1957, Journal Molecular Spectroscopy 1, 124
Breukers R., 1991, PhD Thesis. University of Leiden, Leiden
Buch V., Devlin J.P., 1994, ApJ 431, L135
Bockelée-Morvan D., Brooke T.Y., Crovisier J., 1995, Icarus 116, 18
Caselli P., Hasegawa T.I., Herbst E., 1993, ApJ 408, 548
Charnley S.B., Tielens A.G.G.M., Millar T.J., 1992, ApJ 399, L71
Chiar J.E., Adamson A.J., Kerr T.H., Whittet D.C.B., 1994, ApJ 426, 240
d'Hendecourt L.B., Allamandola, L.J., Baas F., Greenberg J. M., 1982, A&A 109, L12
d'Hendecourt L.B., Allamandola L.J., Greenberg J.M. 1985, A&A 152, 130

d'Hendecourt L.B., Allamandola L.J., Grim R.J.A., Greenberg J.M., 1986, A&A 158, 119
d'Hendecourt L.B., Allamandola L.J., 1986, A&AS 64, 453
Dissly R.W., Allen M., Anicich V.G., 1994, ApJ 435, 685
Ehrenfreund P., Breukers R., d'Hendecourt L., Greenberg J.M., 1992, A&A 260, 431
Ehrenfreund P., Gerakines P.A., Schutte W.A., 1996, in preparation.
Federman S.R., Allen M., 1991, ApJ 375, 157
Fukunaga H., Morokuma K., 1993, Journal Chemical Physics 97, 59
Geballe T.R., 1986a, in: Summer School on Interstellar Processes: Abstracts of Contributed Papers, Hollenbach, D.J., Thronson, H.A. (eds.). NASA, Moffett Field, p. 129.
Geballe T.R., 1986b, A&A 162, 648
Gerakines P.A., Schutte W.A., Greenberg J.M., van Dishoeck E.F., 1995, A&A 296, 810
Gerakines P.A., Schutte W.A., Ehrenfreund P. 1996, submitted to A&A
Glass I.F., 1974, MNRAS 33, 53
Greenberg J.M., 1971, A&A 12, 240
Greenberg J.M., 1973, in: Molecules in the Galactic Environment, Gordon, M.A., & Snyder, L. E. (eds.). Wiley, p.94
Greenberg J.M., 1976, Ap&SS 39, 9
Greenberg J.M., 1979, in: Stars and Star Systems, Westerlund, B.E. (ed.). Reidel, Dordrecht, p. 173.
Grim R.J.A., Greenberg J.M., 1987, ApJ 321, L91
Grim R.J.A., Greenberg J.M., de Groot M.S., Baas F., Schutte W.A., Schmitt B., 1989, A&AS 78, 161
Grim R.J.A., Baas F., Geballe T.R., Greenberg J.M., Schutte W., 1991, A&A 243, 473
Hagen W., Tielens A.G.G.M., Greenberg J.M., 1981, Chemical Physics 56, 367
Hagen W., 1982, Ph.D. thesis. Leiden, University of Leiden
Hasegawa T.I., Herbst E., Leung C.M., 1992, ApJS 82, 167
Hasegawa T.I., Herbst E., 1993a, MNRAS 261, 83
Hasegawa T.I., Herbst E., 1993b, MNRAS 263, 589
Helmich F.P., Jansen D.J., de Graauw Th., Groesbeck T.D., van Dishoeck E.F., 1994, A&A 283, 626
Hiraoka K., Ohashi N., Kihare Y., Yamamoto K., Sato T., Yamashita A., 1994, Chemical Physics Letters 229, 408
Hiraoka K., Yamashita A., Yachi Y., Aruga K., Sato T., 1995, ApJ 443, 363
Hudgins D.M., Sandford S.A., Allamandola L.J., Tielens A.G.G.M., 1993, ApJS 86, 713.
Lacy J.H., Baas F., Allamandola L.J., Persson S.E., McGregor P.J., Lonsdale C.J., Geballe T.R., van de Bult C.E.P., 1984, ApJ 276, 543
Léger A., Jura M., Omont A., 1985, A&A 144, 147
Mathis J.S., Mezger P.G., Panagia N., 1983, A&A 128, 212
Nelander B., 1978, Journal of Molecular Structure 50, 223
Nelander B., 1980, Journal Chemical Physics 72, 77
Okabe H., 1978, Photochemistry of Small Molecules. Wiley, New York
Pendleton, Y.J., Tielens A.G.G.M., Werner, M.W., 1990, ApJ 349, 107
Prasad S.S., Tarafdar S.P., 1983, ApJ 267, 603
Pugh L.A., Rao K.N., 1976, in: Molecular Spectroscopy: Modern Research, Rao, K.N. (ed.). Academic Press, New York, p. 165
Rawlings J.M.C., in: Dust and Chemistry in Astronomy, Millar, T.J., Williams, D.A. (eds.). IOP publishing Ltd., Bristol, p. 219
Sandford S.A., Allamandola L.J., Tielens A.G.G.M., Valero L.J. 1988, ApJ 329, 498
Sandford S.A., Allamandola L.J., Tielens A.G.G.M., Sellgren K., Tapia M., Pendleton Y., 1991, ApJ 371, 607
Sandford S.A., Allamandola L.J., 1993a, ApJ 417, 815
Sandford S.A., Allamandola L.J., 1993b, Sci 262, 400
Schutte W.A., 1988, PhD thesis, University of Leiden, Leiden
Schutte W.A., Tielens A.G.G.M., Allamandola L.J., Cohen M., Wooden D.H., 1990, ApJ 360, 577
Schutte W.A., Greenberg J.M., 1991, A&A 244, 190
Schutte W.A., Tielens A.G.G.M., Sandford S.A., 1991, ApJ 382, 523
Schutte W.A., Allamandola L.J., Sandford S.A., 1993, Icarus 104, 118
Schutte W.A., 1996, in: The cosmic dust connection, Greenberg, J. M. (ed.), in press
Schmitt B., 1994, in: Molecules and grains in space, Nenner, I. (ed.). AIP press, New York, p. 735
Schneider W.G., Bernstein H.J., 1956, Transitions Faraday Society 52, 13
Shalabiea O.M., Greenberg J.M., 1994, A&A 290, 266
Shalabiea O.M., Greenberg J.M., 1995, submitted to A&A
Skinner C.J., Tielens A.G.G.M., Barlow M.J., Justtanont K., 1992, ApJ 399, L79
Smith R.G., Sellgren K., Tokunaga A.T., 1989, ApJ 344, 413
Sternberg A., Dalgarno A., Lepp S., 1987, ApJ 320, 676
Tegler S.C., Weintraub D.A., Rettig T.W., Pendleton Y.J., Whittet D.C.B., Kulesa C.A., 1995, ApJ 439, 279
Tielens A.G.G.M., Hagen W., 1982, A&A 114, 245
Tielens A.G.G.M., Allamandola L.J., 1987a, in: Interstellar Processes, Hollenbach, D. J., Thronson, H. A. (eds.). Reidel, Dordrecht, p. 397
Tielens A.G.G.M., Allamandola L.J., 1987b, in: Physical processes in interstellar clouds, Morfill, G.E., Scholer, M. (eds.). Reidel, Dordrecht, p. 333
Tielens A.G.G.M., 1989, in: IAU symp. 135: Interstellar dust, Allamandola, L.J., Tielens, A.G.G.M. (eds.). Kluwer, Dordrecht, p. 239
Tielens A.G.G.M., Tokunaga A.T., Geballe T.R., Baas F., 1991, ApJ 381, 181
Turner B.E., 1990, ApJ 362, L29
van der Zwet G.P., Allamandola L.J., Baas F., Greenberg J.M., 1985, A&A 145, 262
van Dishoeck E.F., Blake G.A., Draine B.T., Lunine J.I., 1993, in: Protostars and planets III, Levy, E. H., Lunine, J. I. (eds.). The university of Arizona press, Tucson, London, p. 163
Whittet D.C.B., Walker H.J., 1991, MNRAS 252, 63
Whittet D.C.B., 1993, in: Dust and chemistry in astronomy, Millar, T.J., Williams, D.A. (eds.). IOP Publ. Ltd., Bristol, p. 1
Zhao N.S., 1990, PhD thesis. University of Leiden, Leiden

This article was processed by the author using Springer-Verlag TEX A&A macro package 1992.